J Fluoresc (2013) 23:527–532
DOI 10.1007/s10895-013-1186-x

ORIGINAL PAPER

Study of Fluorescence Quenching in Aluminum-Doped Ceria Nanoparticles: Potential Molecular Probe for Dissolved Oxygen

N. Shehata · K. Meehan · D. Leber

Received: 9 August 2012 / Accepted: 24 February 2013 / Published online: 3 March 2013

Abstract This work investigates a novel usage of aluminum-doped ceria nanoparticles (ADC-NPs), as the molecular probe in optical fluorescence quenching for sensing the dissolved oxygen (DO). Cerium oxide (ceria) nanoparticles can be considered one of the most unique nanomaterials that are being studied today due to the diffusion and reactivity of oxygen vacancies in ceria, which contributes to its high oxygen storage capability. Aluminum can be considered a promising dopant to increase the oxygen ionic conductivity in ceria nanoparticles which can improve the sensitivity of ceria nanoparticles to DO. The fluorescence intensity of ADC-NPs, synthesized via chemical precipitation, is found to have a strong inverse relationship with the DO concentration in aqueous solutions. Stern-Volmer constant of ADC-NPs at room temperature is determined to be 454.6 M^{-1}, which indicates that ADC-NPs have a promising sensitivity to dissolved oxygen, compared to many presently used fluorophores. In addition, Stern-Volmer constant is found to have a relatively small dependence on temperature between 25 °C to 50 °C, which shows excellent thermal stability of ADC-NPs sensitivity. Our work suggests that ADC-NPs, at 6 nm, are the smallest diameter DO molecular probes between the currently used optical DO sensors composed of different nanostructures. This investigation can improve the performance of fluorescence-quenching DO sensors for industrial and environmental applications.

Keywords Doped ceria nanoparticles · Oxygen sensor · Fluorescence quenching · Temperature stability

Introduction

The development of fluorescence quenching oxygen sensors has profound effects in the fields of medical science, bioengineering, environmental monitoring, and industrial process control and in military applications [1]. As compared with other types of dissolved oxygen (DO) sensors, such as those that rely on an electrochemical technique, optical sensors have many advantages, which include no or limited oxygen consumption in the sensing process, no requirement for a reference electrode, and immunity to exterior electromagnetic field interference [2]. The majority of fluorescent dyes, mostly organometallic in nature, display oxygen-quenching characteristics, but discrete groups of molecules have shown enhanced sensitivity to oxygen and relatively long fluorescent lifetimes, thus reducing the requirements of the optical transducers [3]. While the detection of dissolved oxygen via fluorescence quenching was demonstrated first in 1939 [4] and sensors based upon this phenomenon are commercially utilized, there continues to be a need to improve the design of the sensors, in particular the sensitivity to DO and thermal stability of the molecular probe, to improve the performance of fluorescence-quenching DO sensors.

Cerium oxide (ceria) nanoparticles can be considered one of the most unique and promising nanomaterials that are being studied today due to the diffusion and reactivity of oxygen vacancies in ceria, which contributes to its high oxygen storage capability [5, 6]. Doped ceria thin films are used as resistive oxygen sensors; however, these resistive

N. Shehata · K. Meehan · D. Leber
Bradley Department of Electrical and Computer Engineering, Virginia Tech, Blacksburg, VA 24060, USA

N. Shehata
Department of Engineering Mathematics and Physics, Faculty of Engineering, Alexandria University, Alexandria 21526, Egypt

N. Shehata (✉)
Virginia Tech, 302 Whittemore (0111), Blacksburg, VA 24061, USA
e-mail: nader83@vt.edu

sensors have similar disadvantages as the sensors based upon electrochemical sensing [7]. As ceria nanoparticles have many of the optical properties desired for the molecular probe in a fluorescence quenching sensor, colloidal ceria nanoparticles doped with aluminum are studied to determine their potential as molecular probes for dissolved oxygen. Aluminum is selected as the dopant since it is proven to increase the ionic conductivity in ceria nanoparticles [8], which can lead to increase the oxygen diffusion constant of this nanomaterial through the charged O-vacancies formed in doped ceria [9]. Consequently, the fluorescence quenching rate constant and the sensitivity of the doped ceria are expected to increase due to their direct proportionality with the ionic diffusion constant [10]. Therefore, ceria nanoparticles doped with aluminum should improve the sensitivity of the fluorescence to the concentration of dissolved oxygen in a colloidal solution as compared to that of undoped ceria nanomaterials. In this work, the fluorescence quenching of ADC-NPs is measured at different DO concentrations at room temperature and different temperatures above the room temperature to study the thermal stability of the sensitivity to DO sensing for ADC-NPs. Our obtained results are compared to the sensitivities and its thermal stability of some presently used fluorophores in DO sensing using fluorescence quenching. This comparison is vital to show the promising sensitivity and its thermal stability of our synthesized ADC-NPs.

Experimental Procedure

Aluminum-doped ceria nanoparticles (ADC-NPs) are synthesized using chemical precipitation, which is preferred over other methods due to its use of inexpensive salt precursors, the simple process that can be performed at or near room temperature and pressure, and the ease at which the process can be scaled for mass production [11]. The synthesis procedure used in this work is similar to that described by Chen and Chang [12]. 0.475 g of cerium (III) chloride heptahydrate (99.9 %, Sigma-Aldrich) and 0.025 mg of aluminum chloride heptahydrate (99.9 %, Sigma-Aldrich) are added in 40 mL de-ionized (DI) water as a solvent. The solution is stirred constantly at rate of 500 rpm in an open container, which has been placed in a 60 °C water bath. After the salts have completely dissolved, 1.6 mL of ammonia is added to initiate the reaction. For the next 2 h, the water bath is maintained at a temperature of 60 °C while the initial product, $Ce(OH)_3$, is converted to Ce_2O_3 [13]. The water bath is then allowed to cool to room temperature and the solution is stirred for an additional 22 h to promote the fracturing of nanorods into nanoparticles. Following the completion of the synthesis process, the colloidal solution is centrifuged and washed with de-ionized water and ethanol to remove any unreacted salts and ammonia and then re-suspended in DI water. This process is done twice. Between both washings, the solution is sonicated to separate any agglomerates. The centrifuged powder is allowed to dry after the second washing.

The experimental setup to measure the fluorescence spectra of the ceria nanoparticles as a function of dissolved oxygen concentration is shown in Fig. 1. 0.2 g of the dried ADC-NP powder is placed in the three holes flask with 200 mL of DI water and sonicated to re-suspend the nanoparticles prior to the fluorescence measurement. The first monochromator (¼m Newport Cornerstone 260) is adjusted to obtain light at a wavelength of 430 nm that is used to optically excite the ADC-NPs in solution. The second monochromator, of similar model to the first one, is positioned at a 90^o angle to the first monochromator to minimize the collection of directly transmitted light and is scanned over the wavelength range from 500 nm to 700 nm. The fluorescence signal from the ADC-NPs is detected by the photomultiplier tube (Newport PMT 77340), inserted at the exit port of the second monochromator, and the intensity spectrum is measured using a power meter (Newport 2935C), connected to the PMT. The dissolved oxygen is controlled using the mass flow rate controller (MKS 247-C), which controls both the inlet flow rate of oxygen and nitrogen to the flask. An independent measurement of the DO concentration is made using a commercial DO meter (Milwaukee MW600) that has a measurement range up to 19.9 mg/L with an accuracy of ±0.1 mg/L.

The synthesized ADC-NPs are imaged using a Philips EM420 transmission electron microscope (TEM), with accelerating voltage of 120 KV, to determine the mean diameter of the formed nanoparticles. Crystallography analysis of the ADC-NPs was performed using a PANalytical X'Pert PRO X-ray diffractometer (XRD) at 45 KV and 40A with Cu K_α radiation (λ=0.154 nm). Also, from the obtained XRD patterns, the mean diameter of the formed nanoparticles can be calculated and compared to the obtained diameter from TEM image for more verification.

To study the impact of temperature on the sensitivity of fluorescence signal from the ADC-NPs in response to the concentration of dissolved oxygen, the three-hole flask is immersed in a water bath on a hot stirrer. The temperature of the water bath is increases from room temperature to 30 °C, then to 40 °C, and finally to 50 °C. In each temperature, the fluorescence spectra are measured at different DO concentrations.

Results and Discussion

Under near UV excitation, the visible fluorescence emission resulted from ADC-NPs is shown in Fig. 2. It can be

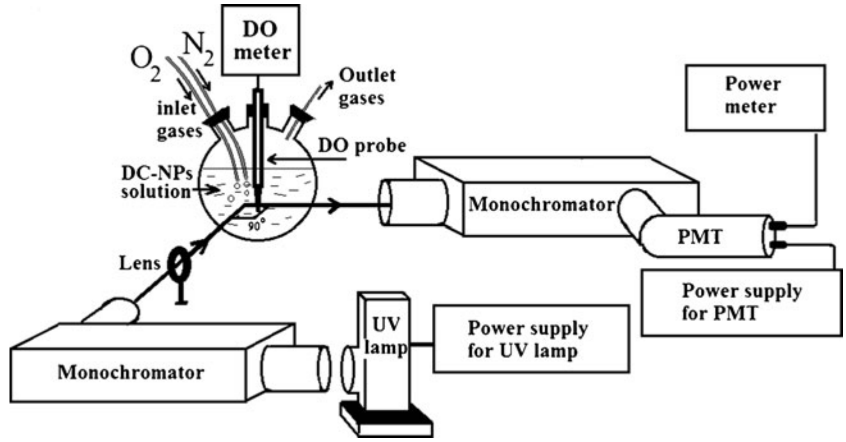

Fig. 1 Experimental apparatus used to measure the fluorescence quenching in ADC-NPs as a function of dissolved oxygen concentration

observed that the amplitude of the emitted signal from the colloidal ADC-NPs decreases by increasing the DO concentration in the aqueous solution. The DO value of 9.2 mg/l is the minimum concentration that we obtained at no added inlet oxygen. We speculate that the reason of that is due to a release of oxygen stored in the ADC-NPs lattice when the nanoparticles are introduced into the solution. This explanation is in agreement to other research work using undoped ceria nanoparticles in optical DO sensing [14]. The relation between the fluorescence intensity and dissolved oxygen concentration is described by Stern-Volmer equation as follows [15]

$$\frac{I_o}{I} = 1 + K_{SV}[O_2] \quad (1)$$

where I_o and I represent the steady-state fluorescence intensity amplitudes in the absence and presence, respectively, of the oxygen quencher, K_{SV} is the Stern–Volmer quenching constant, which is proportional to the sensitivity of the ADC-NPs nanoparticles to sense the dissolved oxygen [16], and $[O_2]$ is the dissolved oxygen concentration. Figure 3 is a plot of I_o/I versus DO concentration when the solution is at room temperature. During the detection of the emitted fluorescence at each stabilized DO concentration, the second monochromator is adjusted at the wavelength of peak intensity; 523 nm, and the power meter records the maximum amplitude for 5 s. Then, the mean value of the maximum amplitudes obtained in this time period is calculated and the error bars shown in Fig. 3 represents the minimum and maximum amplitudes of the peak fluorescence intensity around the mean value. K_{SV} is calculated from the slope of line obtained from a linear fit of the mean amplitudes of peak fluorescence intensity as a function of DO concentration and is found to be 454.6 M^{-1}. The value of K_{SV} for ADC-NPs is much higher than the Stern-Volmer constant of several of the fluorophores commonly used in fluorescence quenching DO sensors. For example, the K_{SV} of PtOEP has a range from 1.4 to 50 M^{-1}, depending on the solution [17, 18], and the published values for K_{SV} of tris (2,2A-bipyridyl) dichlororuthenium(II) hexahydrate of range between 115 and 283 M^{-1} [19, 20]. The Stern-Volmer constant for the ADC-NPs is also much higher than the constant of undoped ceria, which is measured as 184.6 M^{-1} [21]. The large values for K_{SV} for both aluminum-doped and undoped ceria nanoparticles can be attributed to ceria's high oxygen storage capability due to the formed O-vacancies associated with Ce^{3+} ionization states [22]. Aluminum, which is incorporated as a trivalent dopant in ceria, increases the concentration of O-vacancies [23] and the mobility of these vacancies, both of which contribute to the increase in the ionic conductivity observed in thin films of Al-doped ceria as compared to films composed of undoped ceria [8]. Therefore, we conclude that the sensitivity of the ADC-NPs to dissolved oxygen can be related to the concentration of O-vacancies in the nanoparticles.

To substantiate this conclusion, we have repeated the same experiment with some lanthanide-doped ceria nanoparticles, synthesized using chemical precipitation where the aluminum chloride heptahydrate is replaced by a similar weight of a lanthanide chloride heptahydrate. The

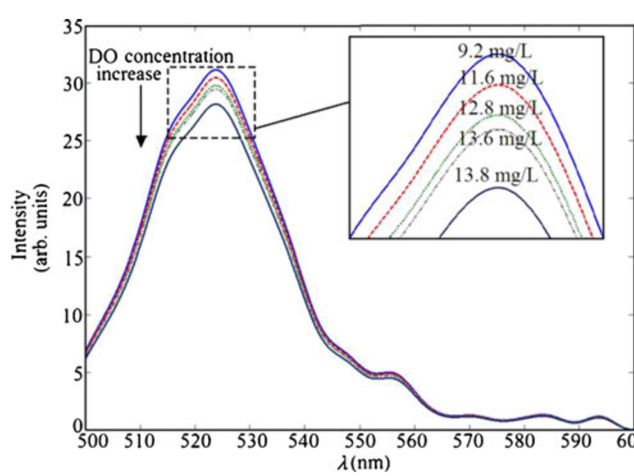

Fig. 2 Fluorescence spectra of the ADC-NPs as a function of DO concentration at room temperature

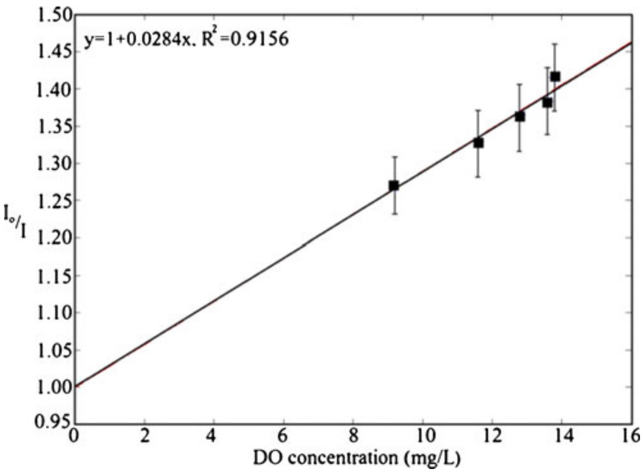

Fig. 3 Ratio of fluorescence intensities, I_o/I, vs. DO concentration for ADC-NPs at room temperature, where the Stern-Volmer constant is the slope calculated from a linear fit of the data

selected lanthanide dopants are two elements that have low association energies with O-vacancies, samarium and neodymium. Both elements have been found to enhance the oxygen ionic conductivity in ceria by increasing the concentration and mobility of O-vacancies [24]. The K_{SV} calculated for samarium-doped ceria is 365 M^{-1} and is 393.5 M^{-1} for neodymium-doped ceria nanoparticles. These results provide support that the sensitivity of aluminum-doped ceria is related to a high concentration of mobile O-vacancies. The sensitivity of the fluorescence in ADC-NPs to DO concentration compared with that of undoped or low activation lanthanides-doped ceria indicates that ADC-NPs has considerable promise as a molecular probe in a fluorescence quenching DO sensor.

A TEM micrograph of the ADC-NPs and associated diffraction rings (inset) is shown in Fig. 4a. The mean diameter of the synthesized ADC-NPs is found to be 6.05 nm and the lattice parameter is 5.53 nm. The X-ray diffraction pattern for the ADC-NPs is shown in Fig. 4b. The first pattern peak is caused by diffraction from the (111) planes in ceria; the (111) planes are the most stable surface plane among the low index planes of ceria [25]. Using data from the first peak, the average particles' diameter can be calculated through Scherrer's formula as follows [26]

$$d = \frac{0.9\lambda}{\beta Cos\theta} \tag{2}$$

where d is the average diameter of the particles, λ is the wave length of X-ray, β is the full-width half-maximum (FWHM) of the surface plane pattern, and θ is the diffraction angle. The average diameter calculated using the XRD data is 5.85 nm which is in good agreement with the averaged diameter calculated from the TEM image. When compared to the sizes of other nanocomposites used as the molecular probes in fluorescence quenching DO sensors, such as Ru(II) tris(4,7 diphenyl- 1,10-phenanthroline) dichloride/silica with a size ranging from 20 to 300 nm and Pt(II) octaethylporphine embedded in xerogel (120–250 nm) [2–27], ADC-NPs can be considered one of the smallest molecular probes for DO sensing.

In the thermal stability study of the ADC-NPs sensitivity to DO, the fluorescence amplitude decreases with increasing temperature when the DO concentration is held constant, as shown in Fig. 5. This is also the trend for fluorescence intensity of undoped ceria, synthesized by the authors within the same experimental procedure, as a function of temperature and is a result of an increase in conversion of ceria from Ce^{3+} ionization state to Ce^{4+} state with elimination of O-vacancies [11]. However, the relative change of fluorescence amplitudes of ADC-NPs at the selected temperatures, compared to room temperature fluorescence amplitude, is found to be lower than the change in fluorescence of

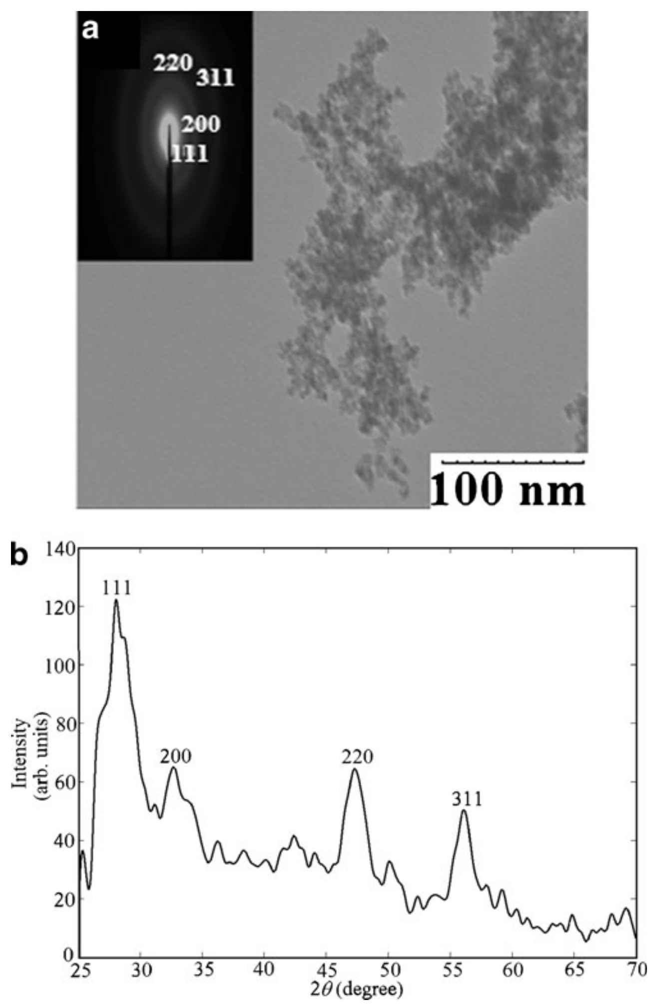

Fig. 4 **a** TEM image of the ADC-NPs with an inset of the electron diffraction pattern and **b**) XRD patterned measured on dried samples of the ADC-NPs

undoped ceria. Since the fluorescence emission of ceria nanoparticles at a specific DO concentration is less temperature dependent when aluminum is used as the dopant, there is a potential to design a fluorescence quenching sensor using ADC-NPs as the molecular probe to measure DO concentrations accurately over a wide temperature range.

The Stern-Volmer constant is calculated using the fluorescence spectra collected at each temperature; the plots of I_o/I vs. DO concentration at 25, 30, 40, and 50 °C are shown in Fig. 6. The calculated values of K_{SV} are 468, 481, and 489.6 M^{-1} at 30, 40, and 50 °C, respectively. It can be noted that the constant, which is proportional to the sensitivity of the fluorescence signal to DO concentration, increases with increasing the temperature. We hypothesize that this is due to the increase in the mobility of O-vacancies, and hence the ionic conductivity [28]. Also, Stokes-Einstein relation states that there is a direct relation between temperature and oxygen diffusion coefficient of the material, which increases Stern-Volmer constant [29]. The increases in K_{SV} at 25, 30, 40, and 50 °C as compared to its value at room temperature (K_{SV}= 454.6 M^{-1}, 25 °C) is 2.95 %, 5.81 %, and 7.69 %, respectively. This can be considered an acceptable stability of ADC-NPs sensitivity for DO sensing with a small variation from the room temperature values, given the significantly larger changes in sensitivity of some of the other fluorescent dyes presently used [30–32]. Also, from our experimental results for undoped ceria and low association lanthanide-doped ceria, these other ceria-based nanomaterials show less thermal stability than ADC-NPS. For example, the K_{SV} for the undoped ceria at 50 °C is 12.68 % larger than the Stern-Volmer constant measured at room temperature. The K_{SV} for samarium-doped ceria at 50 °C shows a change of 28.22 % and neodymium doped ceria has 11.82 % when compared to the values of K_{SV} of these materials measured at room temperature. Thus, the sensitivity of ADC-NPs to DO is more thermally stable than that of the undoped and low association lanthanide-doped ceria nanoparticles.

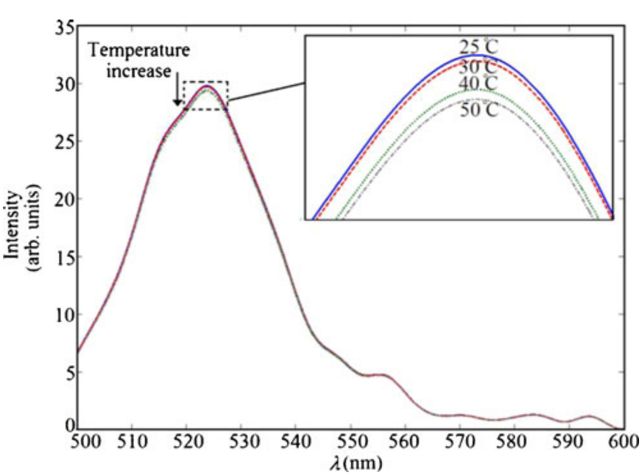

Fig. 5 Quenching of the fluorescence from ADC-NPs with increasing temperature at DO=12.5 mg/L

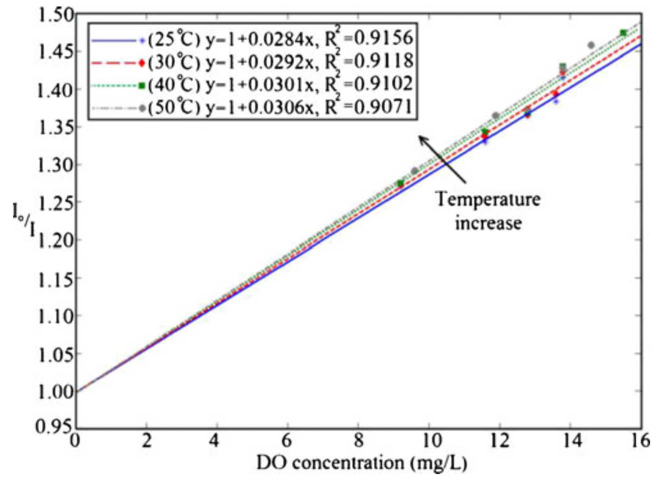

Fig. 6 Ratio of fluorescence intensities, I_o/I, vs. DO concentration for ADC-NPs at 25, 30, 40, and 50 °C

Conclusions

This work introduces a novel investigation of the smallest nanoparticles, 6 nm in diameter of ceria doped with aluminum, that can be used as the molecular probe in optical fluorescence quenching dissolved oxygen sensors. The aluminum dopant in ceria improves the oxygen ionic conductivity and O-vacancies concentration, which is concluded to enhance the sensitivity of this nanomaterial for DO sensing. The ADC-NPs have a high value for K_{SV} and, thus, are more sensitive to the concentration of DO as compared to the K_{SV} calculated for undoped ceria and ceria doped with low association lanthanide (specifically, Sm and Nd) as well as some of the fluorophores presently used in fluorescence quenching DO sensors. The sensitivity of the ADC-NPs studied is shown to have excellent thermal stability with small temperature variations above room temperature compared to other fluorescent dyes as well as compared to undoped, Sm-doped, and Nd-doped ceria. The results of this study show that ADC-NPs have promising application in industrial and environmental dissolved oxygen sensors.

Acknowledgments The authors would like to thank Dr. Niven Monsegue, Dr. Jerry Hunter and Andrew Giordani from the Nanotechnology Characterization and Fabrication Laboratory, Institute of Critical Technologies and Applied Science at Virginia Tech for their training and assistance within characterization measurements. The authors appreciate the support of Dr. Mantu Hudait and Mr. Nikhil Jain with XRD measurements. Also, the authors are grateful to the financial support of the Bradley Department of Electrical and Computer Engineering in Virginia Tech and the Virginia Tech Middle East and North Africa (VT-MENA) program in Egypt.

References

1. Wolfbeis OS (1991) Fiber optic chemical sensors and biosensors. CRC Press, Boca Raton
2. Chu CS, Lo YL (2010) Optical fiber dissolved oxygen sensor based on Pt(II) complex and core-shell silica nanoparticles incorporated with sol–gel matrix. Sensors Actuators B 151:83–89
3. Douglas P, Eaton K (2002) On the inappropriate use of gated emission measurements in oxygen quenching studies of luminescent thin film sensors. Sensors Actuators B 82:48–53
4. Kautsky H (1939) Quenching of luminescence by oxygen. Trans Faraday Soc 35:216–219
5. Basu S, Devi PS, Maiti HS (2004) Synthesis and properties of nanocrystalline ceria powders. J Mater Res 19:3162–3171
6. Lu JL, Gao HJ, Shaikhutdinov S, Freund HJ (2006) Morphology and defect structure of the CeO_2(111) films grown on Ru (001) as studied by scanning tunneling microscopy. Surf Sci 600:5004–5010
7. Sanghavi R, Nandasiri M, Kuchibhatla S, Jiang W, Varga T, Nachimuthu P, Engelhard MH, Shutthanandan V, Thevuthasan S, Kayani A, Prasad S (2011) Thickness dependency of thin-film Samaria-doped ceria for oxygen sensing. IEEE Sensors J 11:217–224
8. Lee JS, Choi KH, Ryu BK, Shin BC, Kim IS (2004) Effects of alumina additions on sintering behavior of gadolinia-doped ceria. Ceram Int 30:807–812
9. Heitjans P, Indris S (2003) Diffusion and ionic conduction in nanocrystalline ceramics. J Phys Condens Matter 15:1257–1289
10. Mills A (1998) Controlling the sensitivity of optical oxygen sensors. Sensors Actuators B 51:60–68
11. Dhannia T, Jayalekshmi S, Kumar M, Rao TP, Bose AC (2009) Effect of aluminum doping and annealing on structural and optical properties of cerium oxide nanocrystals. J Phys Chem Solids 70:1443–1447
12. Chen H, Chang H (2004) Homogeneous precipitation of cerium dioxide nanoparticles in alcohol/water mixed solvents. Colloids Surf A 242:61–69
13. Lawrence NJ, Jiang K, Cheung CL (2011) Formation of a porous cerium oxide membrane by anodization. Chem Commun 47:2703–2705
14. Shehata N, Meehan K, Leber D (2012) Fluorescence quenching in ceria nanoparticles: a dissolved oxygen molecular probe with a relatively temperature insensitive Stern-Volmer constant up to 50 °C. J Nanophotonics 6: 063529/1-11
15. Chu CS, Lo YL (2008) A plastic optical fiber sensor for the dual sensing of temperature and oxygen. IEEE Photon Technol Lett 20:63–65
16. Iosin M, Canpean V, Astilean S (2011) Spectroscopic studies on pH and thermally induced conformational changes of bovine serum albumin adsorbed onto gold nanoparticles. J Photochem Photobiol A 217:395–401
17. Kraker E, Haase A, Lamprecht B, Jakopic G, Konrad C, Köstler S (2008) Integrated organic electronic based optochemical sensors using polarization filters. Appl Phys Lett 92:033302/1-3
18. Shen L, Ratterman M, Klotzkin D, Papautsky I (2011) Use of a low-cost CMOS detector and cross-polarization signal isolation for oxygen sensing. IEEE Sensors J 11:1359–1360
19. Eggins BR (1997) Biosensors: an introduction. John Wiley and Sons, New York
20. Yen DC, Gale BK (2003) An integrated optical oxygen sensor fabricated using rapid-prototyping techniques. Lab Chip 3:297–301
21. Shehata N, Meehan K, Leber D (2012) Dissolved oxygen sensing based on fluorescence quenching of ceria nanoparticles, SPIE Optics and Photonics conference. Nanoscience and Engineering, San Diego, California 4863: 84630/1-9
22. Trovarelli A (2005) Catalysis by ceria and related materials. Imperial College Press, London
23. Skala T, Tsud N, Prince KC, Matolin V (2011) Formation of alumina–ceria mixed oxide in model systems. Appl Surf Sci 257:3682–3687
24. Andersson DA, Simak SI, Skorodumova NV, Abrikosov IA, Johansson B (2006) Optimization of ionic conductivity in doped ceria. PNAS 83:1–4
25. Shehata N, Meehan K, Hudait M, Jain N (2012) Control of oxygen vacancies and Ce+3 concentrations in doped ceria nanoparticles via the selection of lanthanide. J Nanopart Res 14:1173–1183
26. Cullity BD (1956) Elements of x-ray diffraction. Addison-Wesley, Massachusetts
27. Lee YK, Kopelman R (2009) Optical nanoparticles sensors for quantative intracellular imaging. WIREs Nanomed Nanobiotech 1:98–110
28. Damyanova S, Pawelec B, Arishtirova K, Huerta MVM, Fierro JG (2008) Study of the surface and redox properties of ceria-zirconia oxides. Appl Cat A 337:86–96
29. Cappelezzo M, Capellari CA, Pezzin SH, Coelho LAF (2007) Stokes-Einstein relation for pure simple fluids. J Chem Phys 126: 224516-1-224516-5
30. Zhang H, Li B, Lei B, Li W (2008) Oxygen-sensing materials based on $[Ru(bpy)_3]^{+2}$ covalently grafted MSU-3 mesoporous molecular sieves. J Lumin 128:1331–1338
31. Lo YL, Chu CS, Yur JP, Chang YC (2008) Temperature compensation of fluorescence intensity-based fiber-optic oxygen sensors using modified Stern-Volmer model. Sensors Actuators B 131:479–488
32. Shinar R, Zhou Z, Choudhury B, Shinar J (2006) Structurally integrated organic light emitting device-based sensors for gas phase and dissolved oxygen. Anal Chim Acta 568:190–199